Cavity quantum electrodynamics studies with site-controlled InGaAs quantum dots integrated into high quality microcavities

Reitzenstein, S.; Schneider, C.; Albert, F.; Huggenberger, A.; Heindel, T.; Lermer, M.; Stobbe, Søren; Weinmann, P.; Lodahl, Peter; Höfling, S.

Total number of authors:
13

Published in:
Proceedings of SPIE - The International Society for Optical Engineering

Link to article, DOI:
10.1117/12.876794

Publication date:
2011

Document Version
Publisher's PDF, also known as Version of record

Invited Paper

Cavity quantum electrodynamics studies with site-controlled InGaAs quantum dots integrated into high quality microcavities

S. Reitzenstein[1], C. Schneider[1], F. Albert[1], A. Huggenberger[1], T. Heindel[1], M. Lermer[1], S. Stobbe[2], P. Weinmann[1], P. Lodahl[2], S. Höfling[1], M. Kamp[1], L. Worschech[1] and A. Forchel[1]

[1]Technische Physik, Physikalisches Institut, Universität Würzburg, Am Hubland, D-97074 Würzburg, Germany

[2]Department of Photonics Engineering, DTU Fotonik, Technical University of Denmark, Ørsteds Plads 343, DK-2800 Kongens Lyngby, Denmark

e-mail: stephan.reitzenstein@physik.uni-wuerzburg.de

ABSTRACT

Semiconductor quantum dots (QDs) are fascinating nanoscopic structures for photonics and future quantum information technology. However, the random position of self-organized QDs inhibits a deterministic coupling in devices relying on cavity quantum electrodynamics (cQED) effects which complicates, e.g., the large scale fabrication of quantum light sources. As a result, large efforts focus on the growth and the device integration of site-controlled QDs. We present the growth of low density arrays of site-controlled In(Ga)As QDs where shallow etched nanoholes act as nucleation sites. The nanoholes are located relative to cross markers which allows for a precise spatial alignment of the site-controlled QDs (SCQDs) and the photonic modes of high quality microcavites with an accuracy better than 50 nm. We also address the optical quality of the SCQDs in terms of the single SCQD emission mode linewidth, the oscillator strength and the quantum efficiency. A stacked growth of strain coupled SCQDs forming on wet chemically etched nanoholes provide the smallest linewidth with an average value of 210 μeV. Using time resolved photoluminescence studies on samples with a varying thickness of the capping layer we determine a quantum efficiency of the SCQD close to 50 % and an oscillator strength of about 10. Finally, single photon emission with associated with $g^{(2)}(0) = 0.12$ of a weakly coupled SCQD – micropillar system will be presented.

Keywords: Site controlled quantum dots, single photon source, microcavity, quantum dot, quantum efficiency, semiconductor

1. INTRODUCTION

One of the greatest challenges regarding the fabrication of devices based on single semiconductor quantum dots is the precise control of the absolute QD position[1]. Indeed, even though tremendous progress has been achieved in understanding the properties of QDs and integrating them into microcavities, microdiscs or photonic crystals, the random position of self-organized QDs inhibits a large scale fabrication. Thus a great challenge regarding the integration of QDs into devices like single photon sources[2-4], semiconductor building blocks for information processing[5-8] or electron memory modules[9, 10] is the precise control of the position of the QDs. Recently several groups succeeded in the growth of site-controlled QDs and their integration into microcavities[11-17], but a complete characterization of the intrinsic parameters of these dots is still missing.

Here we report on the growth of site-controlled In(Ga)As QDs, their optical properties and their integration into high quality microcavites for cavity quantum electrodynamics experiments. Our technology platform allows for a deterministic fabrication of photonic devices based on single quantum dots and provides an alignment precision better than 50 nm. Besides the technology, we will address the optical quality of the QDs which can be determined by means

Quantum Dots and Nanostructures: Synthesis, Characterization, and Modeling VIII, edited by Kurt G. Eyink, Frank Szmulowicz, Diana L. Huffaker, Proc. of SPIE Vol. 7947, 794702 · © 2011 SPIE · CCC code: 0277-786X/11/$18 · doi: 10.1117/12.876794

of time resolved photoluminescence. By detecting the decay rate of the QD emission as a function of the distance between the QDs and the GaAs-air interface we extract a quantum efficiency of 50% and an oscillator strength of 10 for the excitonic transition of site-controlled QDs. Finally, we will present cQED interaction effects between site-controlled QDs and the photonic modes of high quality microcavites in the weak coupling regime and single photon emission from the coupled system.

2. GROWTH OF SITE CONTROLLED QDS ON PREPATTERNED SUBSTRATES

In this section we present the growth of site controlled In(Ga)As QDs on pre-patterned GaAs substrates. The samples were grown by molecular beam epitaxy (MBE) on (100) oriented GaAs substrates. The substrate is overgrown with a typically 500 nm thick GaAs buffer layer to achieve a high quality surface. Afterwards large (200 µm x 200 µm) square mesa structures and cross marks are realized by optical lithography and plasma etching in a Cl_2/Ar plasma (cf. Fig. 1(a)). The cross marks are later used to retrieve the positions SCQD for device integration[18]. Next, low density arrays of nano-holes are defined on the square mesas using high-resolution electron beam lithography (EBL) and dry etching in a Cl_2/Ar plasma or wet chemical etching (cf. Fig. 1(b)). The resist (Polymethylmethacrylat, PMMA) serves directly as etch mask and is removed after etching using H_2O_2 and H_2SO_4.

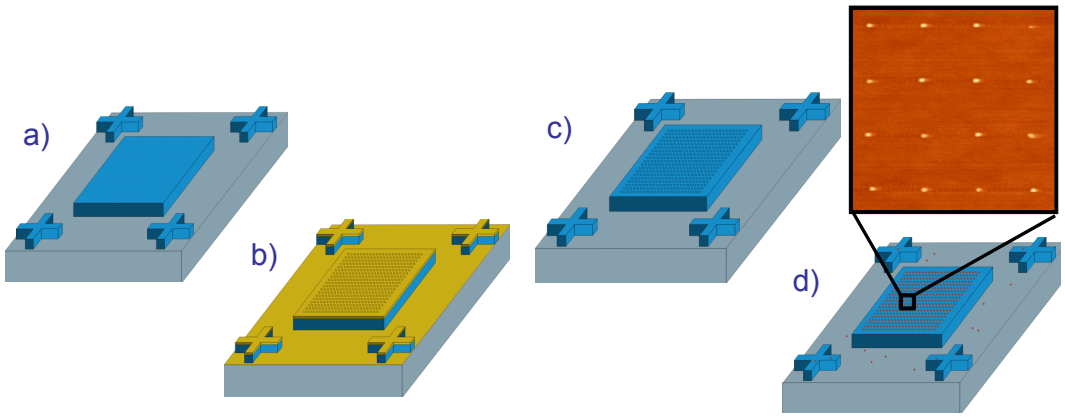

Figure 1. Overview of the SCQD growth process. **(a)** Etching of large square mesas and alignment markers (etching depth approx. 1.5 µm. **(b)** Patterning of nanohole arrays by electron-beam lithography and dry or wet chemical etching. The nanohole act as nucleation centres for the SCQD and are aligned precisely with respect to the alignment markers. **(c)** Removal of etch mask (PMMA) and ex-situ cleaning of the sample. **(d)** In-situ hydrogen assisted cleaning and growth of the SCQDs. Upper part: AFM image of an array of SCQDs with a pitch of 1 µm.

The shallow etched nanoholes which serve as nucleation sites for the subsequent SCQD growth are aligned with respect to the cross markers realized in the first etching step. Thus, individual SCQDs can be retrieved and integrated into single QD based devices. After the processing of the nanohole arrays a careful ex-situ cleaning is performed. It involves a sequence of treatments with pyrrolidon, isopropanol, sulfuric acid, hydrochloric acid, and distilled water. Then the pre-patterned sample is transferred into the load lock chamber of the MBE growth system (cf. Fig. 1(c)), where residual oxides are removed by a surface treatment with activated hydrogen.

Before the growth of the SCQDs growth a thin layer of 8 to 20 nm of GaAs is deposited to smoothen the nanoholes and to obtain monolayer (ML) flat surface. The SCQD are grown under migration enhanced conditions by providing InAs with a nominal growth rate of 0.005 to 0.01 nm/s at a substrate temperature of ~530 °C. Depending on the purpose of the sample a single layer of SCQDs or stacked arrays of SCQDs are grown. For morphology studies of SCQDs in the first InAs layer, sufficient InAs material is deposited to ensure QD nucleation occurs at the etched positions (cf. Fig 1(d)). Such calibration samples are left uncapped for investigations by scanning electron microscopy (SEM) or atomic force microscopy (AFM). Fig. 1(d) (upper part) shows an AFM image of a SCQD sample with a pitch of 1 µm. The ordered growth of the QDs with high yield (larger than 90 %) of occupied nanoholes is clearly seen. It is also noteworthy that there is no signature of QDs at interstitial sites. For optical studies the SCQDs are capped by a GaAs

layer with a thickness larger than 50 nm. Fig. 2 shows excitation power μPL spectra of a single SCQD. At low excitation power we observe excitonic (X) emission. At higher excitation powers further lines appear which are associated with the bi-exciton (XX) and p-shell (X*) emission[19]. The observation of this emission lines is a clear signature of the zero dimensional carrier confinement in the SCQDs. However, the SCQD suffer from linewidths of the excitonic transitions larger than 1 meV. This undesired feature is related to spectral diffusion due to charged carriers at the nanohole interface.

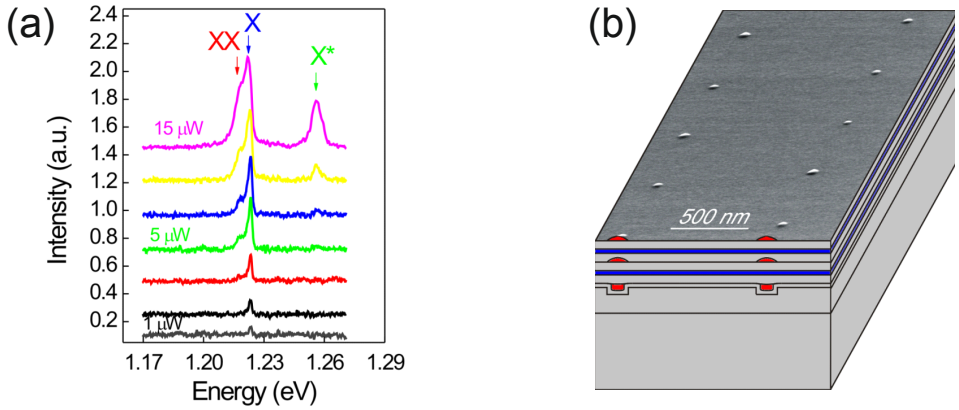

Figure 2. **(a)** Excitation power dependent emission spectra of a site-controlled QD of a sample with a single QD layer. **(b)** Schematic cross section of a sample with stacked layers of SCQDs. The SEM image on top of the sketch shows that excellent ordering of the SCQD is maintained in the stacked layers due to strain coupling of the QDs.

In order to improve the optical quality of SCQDs in terms of the emission linewidth we apply a stack growth of SCQDs to increase the distance to the etched nanohole interface. For this purpose, the first InAs layer is separated by an 8 nm thick GaAs layer from the nanoholes. The nominally supplied thickness of this InAs layer is chosen to be 2.5 MLs. Afterwards, 2 nm of GaAs is deposited and an in-situ annealing step for 2 minutes at 560 °C under arsenic flow is applied. The growth continues with the deposition of a 10 nm thick spacer layer and a second layer of InAs with a nominal thickness of 3.3 MLs. As described above the SCQDs are left uncapped for morphologic investigations. We have realized samples containing up to three layers of InAs in this way. The layer design of the stacked SCQD samples is depicted in Fig. 2(b). As can be seen by the SEM image on top of the sketch, strain coupling ensures that the ordering of the QDs is maintained during the stacked growth of SCQDs. For optical investigations a 100 nm thick GaAs capping layer is deposited. The PCA technique was applied to all layers except the topmost in order to accomplish a spectral detuning between the different layers to facilitate single SCQD studies.

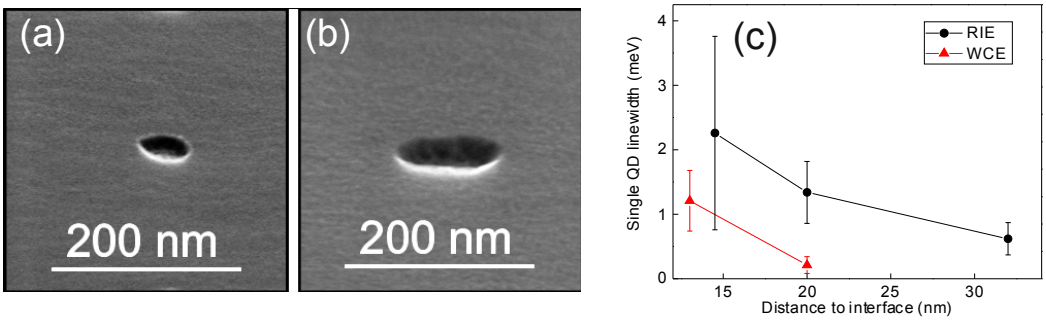

Figure 3. SEM images of nanoholes realized by dry **(a)** and wet chemical **(b)** etching, respectively. **(c)** Single SCQD emission linewidths for SCQD formed on nanoholes prepared by wet chemical etching (WCE) and reactive ion etching (RIE), respectively, as a function of the distance between the SCQD and the nanohole interface.

The samples were investigated by optical spectroscopy in order to assess the effect of a stacked growth of QDs on their emission linewidths[20]. In addition, it was studied whether dry or wet chemical leads to better optical quality of the SCQDs. Figs. 3(a) and (b) show nanoholes realized by dry and wet chemical etching, respectively. In case of dry chemical etching smaller nanoholes can be realized if compared to wet chemically etched one. However, wet chemical etching provides nanoholes with smoother edges. The optical studies revealed a pronounced dependence of the SCQD linewidths on the number of stacks and the etching method. As can be seen in Fig. 3(c) the linewidths of the uppermost SCQD layer decrease from values larger than 2 meV for a sample with a single QD layer down to about 0.7 meV for a sample with three stacks and a correspondingly larger separation (32 nm) between uppermost QD layer and the etched interface. Moreover, we found that the etching method has strong influence on the linewidths of the SCQDs. Significantly smaller linewidths are observed for SCQDs aligned to nanoholes realized by wet chemical etching. For this etching procedure a statistical analysis reveals an average linewidth of 210 μeV for SCQD in the second layer of a stacked sample.

3. QUANTUM EFFICIENCY AND OSCILLATOR STRENGTH OF SITE CONTROLLED QDS

In this section we will address the quantum efficiency and the oscillator strength of site-controlled QDs. For this purpose we apply a method introduced by Drexhage, who demonstrated a modified decay rate for fluorescing molecules close to a reflecting surface[21]. Basically the method considers that the radiative decay rate is modified in the proximity of the interface. This leads to a characteristic oscillation of the local density of optical states (LDOS) at the position of the QDs when varying the thickness of the GaAs capping layer[22, 23]. Consequently, the radiative decay rate of the QDs shows also an oscillatory variation as a function of the distance z to the interface (cf. Fig. 4 (a)). In contrast, the non-radiative decay is not affected by a change of the LDOS. Hence, time-resolved measurements on SCQD samples with varying thickness of the capping layers allows one to extract the non-radiative (Γ_{nrad}) and radiative (Γ_{rad}^{hom}) decay rates of the QDs separately which allows one to determine the QE and the OS (f) of the SCQDs via

$$QE = \frac{\Gamma_{rad}^{hom}}{\Gamma_{rad}^{hom}+\Gamma_{nrad}}, \quad (1)$$

$$f(\omega) = \frac{6\, m_e \epsilon_0 \pi c_0^3}{q^2 n \omega^2}\, \Gamma_{rad}^{hom}(\omega). \quad (2)$$

Here m_e denotes the electron mass, q the electron charge, e_0 the dielectric constant, c_0 the velocity of light, n the refractive index and ω the angular emission frequency.

These parameters were determined for In(Ga)As SCQDs grown by MBE on a GaAs (100) wafer as detailed above. In addition, a distributed Bragg reflector (DBR) consisting of 6 pairs of quarter wavelength thick GaAs and AlAs layers was included below the active layer. The DBR was designed to reflect the emission from the SCQDs to ensure enhanced intensity in time resolved photoluminescence (PL) experiments. We prepared a sample with SCQD arrays with a pitch of 1 μm and a lateral extension of 200 μm x 200 μm where the nanoholes were prepared by high resolution electron beam lithography and wet chemical etching. The samples include two strain coupled InAs layers. The first InAs layer does not form optically active QDs but previous studies showed its importance for the formation of the SCQDs in the second InAs layer[24].

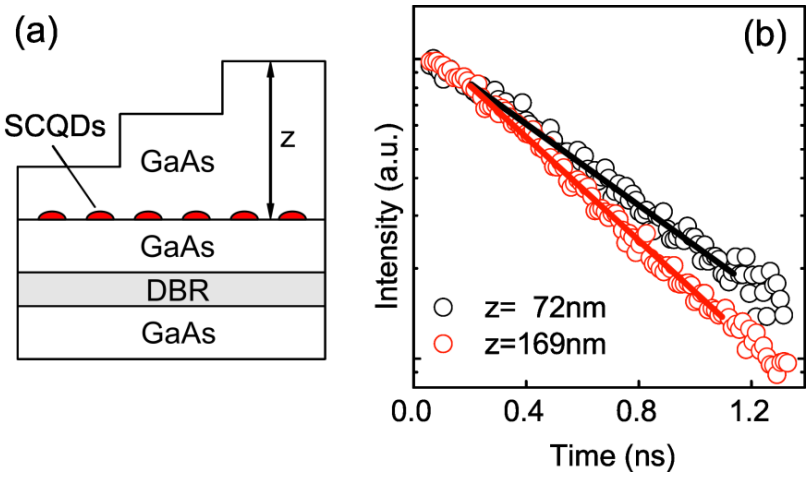

Figure 4. (**a)** Schematic view of the sample layout to determine the QE and OS under variation of the capping thickness *z*. **(b)** PL decay curves for thicknesses of the capping layer of 72 nm and 169 nm, respectively.

Subsequent to the growth the wafer was cleaved into 13 pieces each of which contains one 200 µm x 200 µm wide array of SCQDs (pitch: 1 µm). Using wet chemical etching technique we obtained 13 SCQD samples with capping layers between 37 nm and 283 nm by a variation of the etching time. Cross-sectional scanning electron microscopy was applied to determine the actual thickness of the capping layer. Time-resolved PL studies were performed at 10 K in a standard PL configuration. The SCQDs were excited by a mode-locked Ti:sapphire laser emitting 150 fs wide pulses at a repetition rate of 82 MHz and a wavelength of 780 nm. The PL setup provides a spectral resolution of 150 µeV and a temporal resolution of 100 ps using a microchannel plate as detector.

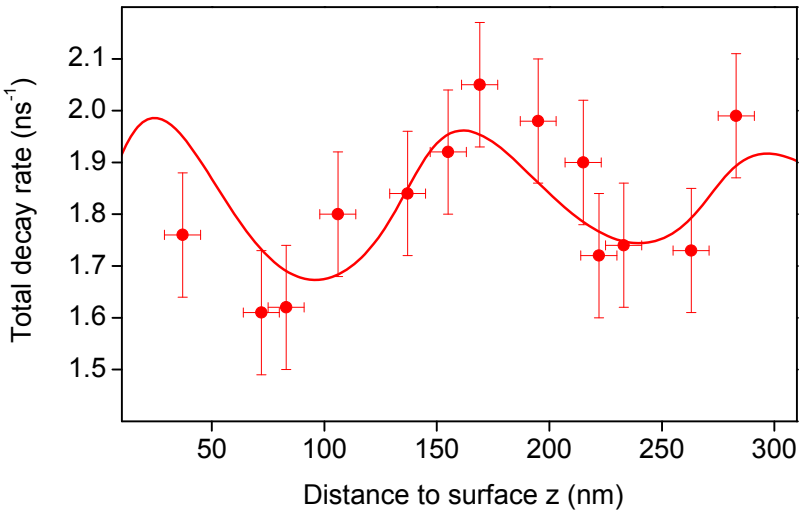

Figure 5. Total PL decay rate of an ensemble of SCQDs as a function of the capping layer thickness *z*.

To access the optical quality of the SCQDs in terms of the QE and OS we studied their decay characteristics under variation of z for the central wavelength (930 nm) of the inhomogeneously broadened emission band. Fig. 4(b) shows characteristic PL decay curves from SCQDs two different capping layer thicknesses (z = 72 nm and 169 nm) on a semi-logarithmic scale (detection window: (930 ± 2) nm). The total decay rates of the bright excitons are obtained by fitting

the data at short delay times with an exponential decay function (solid black and solid red/gray lines in Fig. 4(b)). We obtain total decay rates of 1.61 ns^{-1} for z = 72 nm and 2.05 ns^{-1} for z = 169 nm. In the same way we determined the total decay rate for all 13 samples and plotted them in Fig. 5 versus *z*. As expected from theory a clear oscillatory behavior is observed.

The QE and OS of the SCQDs were determined by comparing the measured decay rates to the LDOS following the procedure outlined in Ref. [23]. It is important to note that in the present case the DBR stack and the buffer layers containing AlGaAs sections must be taken into account to calculate the LDOS. From the fits of the experimental data presented in Fig. 5 to the calculated LDOS we have extracted the decay rates $\Gamma_{rad}^{hom} = (0.90 \pm 0.20)\, n^{-1}$ and $\Gamma_{nrad} = (0.99 \pm 0.20)\, n^{-1}$. Taking Eqs. (1) and (2) into account we obtain QE = (48 ± 14) % and f = 10.1 ± 2.6, respectively. The OS compares well with values on the order of 10 reported for standard InAs QDs. Even though the QE is lower than values exceeding 90 % of self-assembled QDs[22] the present result is very encouraging with respect to the further development of SCQDs. The lower QE is attributed to a tunnelling of carriers confined in the SCQD to the etched nanohole surface and a subsequent non-radiative recombination at midgap interface states[24]. Thus, the QE of SCQDs could be enhanced by optimizing the properties of the buffer layer between the SCQDs and the nanohole interface.

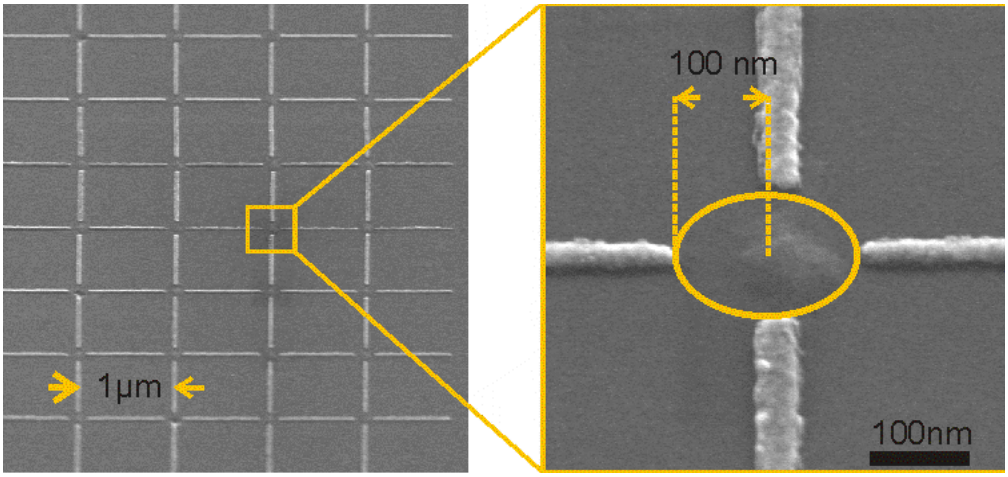

Figure 6. SEM images of a test structure which demonstrates an alignment accuracy of about 50 nm for crosshair markers aligned to SCQDs with a pitch of 1 µm.

4. SINGLE PHOTON EMISSION FROM A SITE-CONTROLLED QD INTEGRATED INTO A MICROPILLAR CAVITY

In this section we describe the integration of SCQD into micropillar cavities and cQED effects as well as single photon emission from such a system. In the present work we focus on light-matter interaction effects in the weak coupling regime. The associate Purcell factor F_P is given by[25]

$$F_P = \frac{\tau_{3D}}{\tau_{cavity}} \propto \frac{Q}{V_{mode}} \left| \frac{E(\vec{r})}{E_{max}} \right|^2, \qquad (3)$$

where τ_{3D} (τ_{cavity}) denotes the spontaneous emission lifetime of the emitter in bulk material (in the microcavity), Q the quality factor of the microcavity with a mode volume V_{mode}, E_{max} the maximum intensity of the confined electrical field and $E(\vec{r})$ the fied intensity at the position $\vec{r}$. Moreover, we need to consider that the extraction efficiency η_{ext} of a micropillar based single photon source relying on cQED effects depends via

$$\eta_{ext} = \frac{Q}{Q_{2D}}\,\beta = \frac{Q}{Q_{2D}}\,\frac{F_P}{F_P+1} \qquad (4)$$

on the Purcell factor, where Q_{2D} is the Q-factor of the planar microcavity. Thus, it is crucial to control the position of the emitter – the QD in our case – which should be placed at the field maximum in order maximise the Purcell factor and the extraction efficiency, respectively. In order to position SCQD in spatial resonance with the cavity mode we employ the cross markers defined together with the square mesas as detailed in section 2. For thin overgrowth thicknesses a standard deviation from the target position of ~50 nm could be demonstrated by patterning crosshair markers aligned to SCQDs as shown exemplarily in Fig. 6. This technology platform allowed for the deterministic integration of SCQD into photonic crystal cavities[26]. The integration of SCQDs into micropillar cavities is very challenging since for rather high epitaxial overgrowth thicknesses of the upper DRB as needed for micropillar cavities the alignment procedure is complicated by the smeared out edges of the alignment marks. Nevertheless, because these deviations occur in a symmetric way we can still obtain a reasonable good alignment even after a DBR section of 2 μm thickness. The alignment accuracy was tested for reference micropillars for which SCQDs have been positioned at the top facet of the structure. Fig. 7(a) shows an SEM of such a micropillar with an SCQD placed nominally in the center of the upper facet. It is clearly seen that an alignment accuracy better than 100 nm can be achieved for this process.

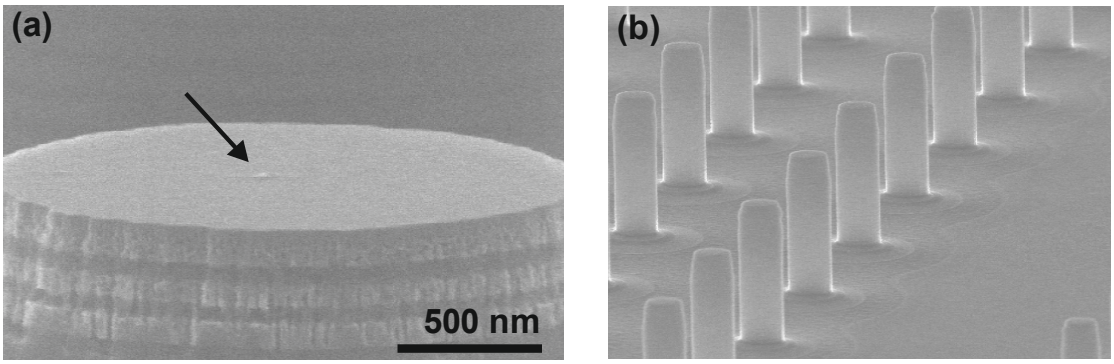

Figure 7. (**a)** SEM of a reference micropillar with a single positioned SCQD (indicated by an arrow). **(b)** SEM image of an array of fully processed micropillar, each of which contains a single positioned SCQD in the active layer.

We will now address the growth and optical properties of SCQDs integrated into micropillar cavities. In order to optimize the optical quality of the SCQDs, three layers of InAs were stacked on top of the nanoholes. As confirmed by atomic force microscopy (AFM) image on uncapped SCQDs, well ordered QD arrays have been obtained also for three stacked InAs layers (not shown)[27]. The growth of the SCQD on the nanohole arrays was initiated by an 8 nm thick GaAs buffer layer followed by the first InAs layer. The second and third InAs layers were separated by a barrier with a thickness of 10 nm each. Both, the first and the second InAs layer were capped by 2 nm of GaAs followed by an in-situ annealing step at 560 °C for 2 minutes. This particular growth routine shifts the emission of the QDs in the first and second layer towards higher energies which allows us to spectrally detune their emission from those SCQDs located in the topmost third layer envisaged for the coupling to the resonator[28]. cQED interaction effects are demonstrated in a spatially resonant SCQD-micropillar cavity system. For this purpose we integrated a stack of three InAs layers as described above in the active region of a planar AlAs/GaAs microcavity structure. The one-λ GaAs cavity is sandwiched between 25 AlAs/GaAs mirror pairs in the bottom DBR and 12 mirror pairs in the top DBR. Afterwards arrays of micropillars with deterministically placed SCQD were patterned using high-resolution electron beam lithography and plasma etching in an ECR etching system. Fig. 7(b) shows an SEM image of an array of such SCQD-micropillar cavities.

Spatially resonant QD-micropillar systems were investigated at low temperature (10 to 50 K) by means of micro-photoluminescence (μPL) spectroscopy. Each processed micropillar with a diameter below 2 μm patterned on a SCQD array with a period of 1 μm is expected to contain with high probability > ~90 % only one single SCQD emitting at about 960 nm. cQED effects are investigated by temperature tuning of single SCQD emission lines through resonance with the cavity mode of a micropillar with a diameter of 1.0 μm and a Q-factor of 1700. The corresponding μPL intensity map is depicted in Fig. 8. From this plot it is obvious that the X transition of the SCQD is already resonant with the fundamental cavity mode at low temperature, whereas the X+ transition can be tuned through the resonance by increasing the temperature. The characteristic enhancement of emission on spectral and spatial resonance is a clear signature of a weakly coupled SCQD-micropillar cavity system. We attribute the occurrence of several emission lines in a spectral range of a few meV to the excitonic (X), positively charged (X^+) and the biexcitonic (XX) emission of one single SCQD, as supported by power dependent measurements (not shown). We would like to point out that the cavity emission is almost absent under weak excitation conditions when no transition line of the SCQD is on resonance with the cavity mode. This is a clear advantage of the SCQD-microcavity system. Indeed, microcavites with standard self-assembled QDs suffer typically from strong uncorrelated background emission from a large number of off-resonant QDs illuminating the cavity mode which is detrimental with respect to single photon sources with a low multiphoton emission probability.

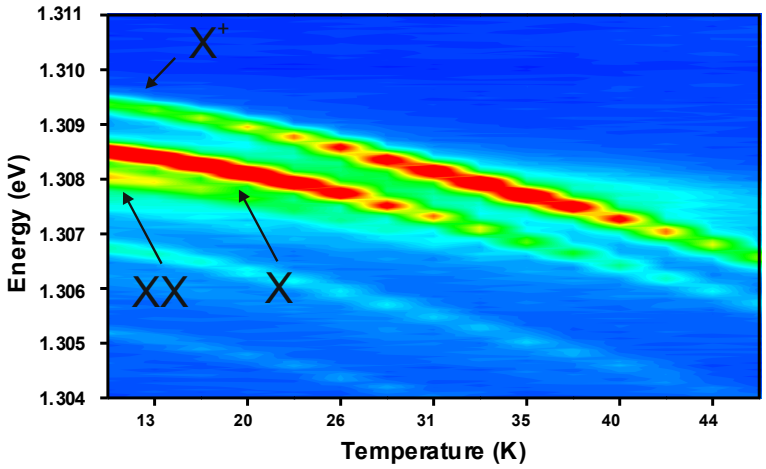

Figure 8. μPL intensity map showing the temperature tuning of single SCQD emission lines (X, XX and X^+) through resonance with the fundamental cavity mode of a micropillar with a diameter of 1.0 μm and a Q-factor of 1700. Red colour indicates high intensity. On resonance a strong enhancement of emission is observed due to the Purcell-effect.

Finally we prove the feasibility of a coupled SCQD-micropillar system to act as a single photon source. For this purpose, we performed photon autocorrelation measurements using a fiber coupled Hanbury-Brown and Twiss setup. The SCQD are excited by a mode locked Ti:Sapphire laser in fs-mode at a repetition rate of 82 MHz which was tuned to an emission wavelength of 760 nm. The photon statistics of the cavity emission was probed for X^+ being on resonance with the cavity mode. The corresponding second order autocorrelation function $g^{(2)}(\tau)$ is presented in Fig. 9. The system shows pronounced antibunching as expected from a non-classical light source. In fact, the observed value of $g^{(2)}(0) = 0.12 < 0.5$ is a clear signature of single photon emission with a low multi-photon emission probability. This is result is very promising with respect to the application and integration of SCQD in scalable quantum light sources.

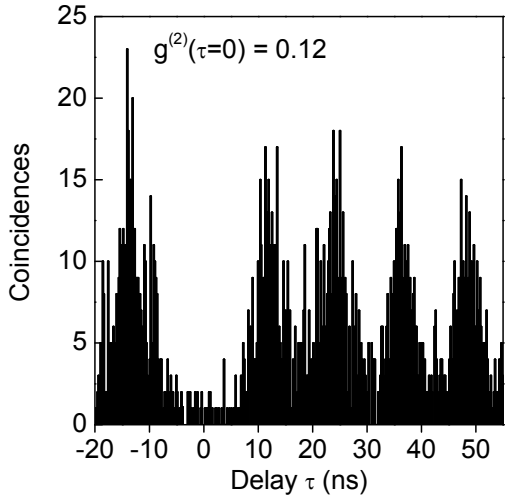

Figure 9. Photon autocorrelation function $g^{(2)}(\tau)$ of a single SCQD transition (X^+, cf. Fig. 9) on resonance with the fundamental cavity mode of a micropillar cavity with a diameter of 1.0 μm and a Q-factor of 1700.

5. CONCLUSIONS

In conclusion we have demonstrated the growth of site-controlled InGaAs QDs. The SCQDs nucleate on shallow etched nanohole arrays which are positioned with respect the cross markers in order to retrieve the dot positions for device integration with an alignment accuracy better than 50 nm. An optimized growth procedure based on wet chemically etched nanoholes and a stacked layers of strain coupled SCQD allowed us to demonstrate a highly order formation of QDs with high yield and enhanced optical properties in terms of the single QD linewidths and the quantum efficiency which is as large as 50 % for the present technology. The SCQDs were integrated into micropillar cavities to obtain spatially and spectrally resonant systems which feature light-matter interaction effects in the weak coupling regime and clear single photon emission associated with $g^{(2)}(0)$=0.12. These results are very promising with respect to future scalable and deterministic quantum light sources and they will pave the way for electrically pumped single photon sources based in SCQDs, strongly coupled SCQD – microcavity systems and microlasers with a defined number of emitters in the active layer.

ACKNOWLEDGEMENTS

The authors thank M. Emmerling and A. Wolf for expert sample preparation. Financial support by the German Ministry of Education and Research (BMBF) within the project "QuaHL-rep", the Deutsche Forschungsgemeinschaft (DFG) within the project FO 146/14-1 "Single quantum dot lasers" and by the European Commission (EC) within the IST-project "QPhoton" is gratefully acknowledged.

REFERENCES

[1] Michler, P., "Single Quantum Dots: Fundamentals, Applications and New Concepts," Springer, Berlin, 2003
[2] Michler, P., Kiraz, A., Becher, C., Schoenfeld, W. V., Petroff, P. M., Zhang, L. D., Hu, E. and Imamoglu, A., „A Quantum Dot Single-Photon Turnstile Device," Science **290**, 2282 (2000).
[3] Pelton, M., Santori, C., Vuckovic, J., Zhang, Y. B., Solomon, G. S., Plant, J. and Yamamoto, Y., "Efficient Source of Single Photons: A Single Quantum Dot in a Micropost Microcavity," Phys. Rev. Lett. **89**, 233602 (2002).
[4] Yuan, Z. L., Kardynal, B. E., Stevenson, R. M., Shields, A. J., Lobo, C. J., Cooper, K., Beattie, N. S., Ritchie, D. A. and Pepper, M., "Electrically Driven Single-Photon Source," Science **295**, 102 (2002).
[5] Zrenner, A., Beham, E., Stufler, S., Findeis, F., Bichler, M. and Abstreiter, G., „7.Coherent properties of a two-level system based on a quantum-dot photodiode," Nature (London) **418**, 612 (2002).

[6] Li, X. Q., Wu, Y. W., Steel, D., Gammon, D., Stievater, T. H., Katzer, D. S., Park, D., Piermarocchi, C. and Sham, L. J., "An All-Optical Quantum Gate in a Semiconductor Quantum Dot," Science **301**, 809 (2003).
[7] Reithmaier, J. P., Sek, G., Löffler, A., Hofmann, C., Kuhn, S., Reitzenstein, S., Keldysh, L. V., Kulakovskii, V. D., Reinecke, T. L. and Forchel, A., „Strong coupling in a single quantum dot–semiconductor microcavity system," Nature (London) **432**, 197 (2004).
[8] Yoshie, T., Scherer, A., Hendrickson, J., Khitrova, G., Gibbs, H. M., Rupper, G., Ell, C., Shchekin, O. B. and Deppe, D. G., „7.Vacuum Rabi splitting with a single quantum dot in a photonic crystal nanocavity," Nature (London) **432**, 200 (2004).
[9] Kroutvar, M., Ducommun, Y., Heiss, D., Bichler, M., Schuh, D., Abstreiter, G. and Finley, J. J., „3.Optically programmable electron spin memory using semiconductor quantum dots," Nature (London) **432**, 81 (2004).
[10] Schliemann, A., Worschech, L., Reitzenstein, S., Kaiser, S. and Forchel, A., „Large threshold hysteresis in a narrow AlGaAs/GaAs channel with embedded quantum dots," Appl. Phys. Lett. **81**, 2115 (2002).
[11] Schmidt, O. G., "Lateral Alignment of Epitaxial Quantum Dots," Springer, Berlin, (2007).
[12] Nakamura, Y., Schmidt, O. G., Jin-Phillipp, N. Y., Kiravittaya, S., Muller, C., Eberl, K., Grabeldinger, H. and Schweizer, H., „Vertical alignment of laterally ordered InAs and InGaAs quantum dot arrays on patterned (001) GaAs substrates," J. Cryst. Growth **242**, 339 (2002).
[13] Song, H. Z., Usuki, T., Hirose, S., Takemoto, K., Nakata, Y., Yokoyama, N. and Sakuma, Y., "Site-controlled photoluminescence at telecommunication wavelength from InAs/InP quantum dots," Appl. Phys. Lett. **86**, 113118 (2005).
[14] Atkinson, P., Ward, M. B., Bremner, S. P., Anderson, D., Farrow, T., Jones, G. A. C., Shields, A. J. and Ritchie, D. A., "Site-Control of InAs Quantum Dots using Ex-Situ Electron-Beam Lithographic Patterning of GaAs Substrates," Jpn. J. Appl. Phys., Part 1 **45**, 2519 (2006).
[15] Baier, M. H., Watanabe, S., Pelucchi, E. and Kapon, E., "High uniformity of site-controlled pyramidal quantum dots grown on prepatterned substrates," Appl. Phys. Lett. **84**, 1943 (2004).
[16] Portavoce, A., Hull, R., Reuter, M. C. Ross, F. M., "Nanometer-scale control of single quantum dot nucleation through focused ion-beam implantation," Phys. Rev. B **76**, 235301 (2007).
[17] Tran, T., Muller, A., Shih, C. K., Wong, P. S., Balakrishnan, G., Nuntawong, N., Tatebayashi, J. and Huffaker, D. L., "Single dot spectroscopy of site-controlled InAs quantum dots nucleated on GaAs nanopyramids," Appl. Phys. Lett. **91**, 133104 (2007).
[18] Schneider, C., Strauß, M., Sünner, T., Huggenberger, A., Wiener, D., Reitzenstein, S., Kamp, M., Höfling, S. and Forchel, A., „Lithographic alignment to site-controlled quantum dots for device integration," Appl. Phys. Lett. **92**, 183101 (2008).
[19] Alloing, B., Zinoni, Z., Zwiller, V., Li, L. H., Monat, C., Gobet, M., Buchs, G., Fiore, A., Pelucchi, E. and Kapon, E., „Growth and characterization of single quantum dots emitting at 1300 nm, " Appl. Phys. Lett. **86**, 101908 (2005).
[20] Schneider, C., Huggenberger, A., Sünner, T., Heindel, T., Strauß, M., Göpfert, S., Weinmann, P., Reitzenstein, S., Worschech, L., Kamp, M., Höfling S. and Forchel, A., „Single site-controlled In(Ga)As/GaAs quantum dots: growth, properties and device integration ," Nanotechnology **20**, 434012 (2009).
[21] Drexhage, H., „Influence of a dielectric interface on fluorescence decay time," J. Lumin. **1-2**, 693 (1970).
[22] Johansen, J., Stobbe, S., Nikolaev, I. S., Lund-Hansen, T., Kristensen, P. T., Hvam, J. M., Vos, W. L. and Lodahl, P., „Size dependence of the wavefunction of self-assembled InAs quantum dots from time-resolved optical measurements," Phys. Rev. B **77**, 073303 (2008).
[23] Stobbe, S., Johansen, J., Kristensen, P. T., Hvam, J. M. Lodahl, P., „Frequency dependence of the radiative decay rate of excitons in self-assembled quantum dots: Experiment and theory," Phys. Rev. B **80**, 155307 (2009).
[24] Albert, F., Stobbe, S., Schneider, C., Heindel, T., Reitzenstein, S., Höfling, S., Lodahl, P., Worschech, L. and Forchel, A., „Quantum efficiency and oscillator strength of site-controlled InAs quantum dots," Appl. Phys. Lett. **96**, 151102 (2010).
[25] Barnes, W. L., Björk, G., Gérard, J. M., Jonsson, P., Wasey, J. A. E., Worthing, P. T. and Zwiller, V., "Solid-state single photon sources: light collection strategies," Eur. Phys. J. D **18**, 197 (2002).
[26] Sünner, T., Schneider, C., Strauß, M., Huggenberger, A., Wiener, D., Höfling, S., Kamp, M. and Forchel, A., „Scalable fabrication of optical resonators with embedded site-controlled quantum dots," Opt. Lett. **33**, 1759-1761 (2008).

[27] Schneider, C., Heindel, T., Huggenberger, A., Weinmann, P., Kistner, C., Kamp, M., Reitzenstein, S., Höfling, S., and A. Forchel, „Single photon emission from a site-controlled quantum dot-micropillar cavity system," Appl. Phys. Lett. **94**, 111111 (2009).
[28] Wang, L., Rastelli, A. and Schmidt, O. G., „Structural and optical properties of In(Ga)As/GaAs quantum dots treated by partial capping and annealing," J. Appl. Phys, **100**, 064303 (2006).